Proc. Natl. Acad. Sci. USA
Vol. 92, pp. 3156–3160, April 1995
Neurobiology

Quantitative measurement of intraorganelle pH in the endosomal–lysosomal pathway in neurons by using ratiometric imaging with pyranine

CAROLINE C. OVERLY*†, KYUNG-DALL LEE*, ERIC BERTHIAUME‡, AND PETER J. HOLLENBECK*†

*Department of Neurobiology, †Program in Neuroscience, and ‡Department of Cell Biology, Harvard Medical School, 220 Longwood Avenue, Boston, MA 02115

Communicated by Gerald D. Fischbach, Harvard Medical School, Boston, MA, December 27, 1994

ABSTRACT **Organelle acidification is an essential element of the endosomal–lysosomal pathway, but our understanding of the mechanisms underlying progression through this pathway has been hindered by the absence of adequate methods for quantifying intraorganelle pH. To address this problem in neurons, we developed a direct quantitative method for accurately determining the pH of endocytic organelles in live cells. In this report, we demonstrate that the ratiometric fluorescent pH indicator 8-hydroxypyrene-1,3,6-trisulfonic acid (HPTS) is the most advantageous available probe for such pH measurements. To measure intraorganelle pH, cells were labeled by endocytic uptake of HPTS, the ratio of fluorescence emission intensities at excitation wavelengths of 450 nm and 405 nm (F450/405) was calculated for each organelle, and ratios were converted to pH values by using standard curves for F450/405 vs. pH. Proper calibration is critical for accurate measurement of pH values: standard curves generated *in vitro* yielded artifactually low organelle pH values. Calibration was unaffected by the use of culture medium buffered with various buffers or different cell types. By using this technique, we show that both acidic and neutral endocytically derived organelles exist in the axons of sympathetic neurons in different steady-state proportions than in the cell body. Furthermore, we demonstrate that these axonal organelles have a bimodal pH distribution, indicating a rapid acidification step in their maturation that reduces the average pH of a fraction of the organelles by 2 pH units while leaving few organelles of intermediate pH at steady state. Finally, we demonstrate a spatial gradient of organelle pH along axons, with the relative frequency of acidic organelles increasing with proximity to the cell body.**

Organelle contents acidify as they progress through the endosomal–lysosomal pathway (1), but the nature of the progression is not well understood. In addition, little is known about this degradative pathway in neuronal cells (2, 3). To study the spatiotemporal organization of this dynamic process in neurons requires a noninvasive method for measuring organelle pH in live cells. Most studies of intracellular pH have focused on the cytoplasm (e.g., refs. 4–9; for review, see ref. 10), and considerably less work has addressed the pH of organelles within living cells (11–13). On the latter subject, the extant literature suffers from the use of pH probes that are nonquantitative, subject to a variety of artifacts, impossible to calibrate accurately, or restricted to use in fixed cells. Here we present an accurate quantitative method for determining intraorganelle pH in living cells that is ideal for studies of the endosomal–lysosomal pathway in neurons and other cell types.

Our work employs the fluorescent pH indicator 8-hydroxypyrene-1,3,6-trisulfonic acid (HPTS) that has six properties essential for studies of intraorganelle pH: (*i*) It lacks toxicity or interference with normal cellular functions at the experimental concentrations. (*ii*) It has a pKa near neutrality and high pH resolution in the physiologic range. (*iii*) It responds rapidly to changes in pH. (*iv*) It is a ratiometric indicator, allowing quantitative measurements regardless of organelle size or probe concentration. (*v*) It can be calibrated within live cells, for precise and accurate quantification. (*vi*) It is hydrophilic and membrane impermeant, allowing easy loading into endosomes by fluid-phase endocytosis but preventing leakage across intracellular membranes. The latter property is particularly important in studies of neurons, since a marker endocytosed at the axonal tip must be retained within organelles for a relatively long period while the organelles undergo retrograde transport over considerable distances. HPTS has been recognized as a useful probe for dynamic pH measurements of membrane-bound aqueous medium (14, 15) and, in principle, as the best fluorescent indicator for the measurement of pH in the physiologic range due to its vastly greater accuracy and sensitivity compared to commonly used pH indicators (16). However, HPTS has not been exploited for cell biological studies, perhaps because the lack of a hydrolyzable membrane permeant analog precludes easy analysis of cytoplasmic pH.

In this study, we present detailed data on the proper use of HPTS for the study of organelle acidification in the endosomal–lysosomal pathway and insights into the kinetics of organelle acidification and the spatial organization of this pathway in neuronal cells. We demonstrate that for accurate pH measurements using HPTS, calibration must be done *in situ*, not *in vitro*, and at the time of experimental data collection. Our experimental data demonstrate that organelles in the endosomal–lysosomal pathway do become acidified within the axons of cultured sympathetic neurons and that their pH distribution is distinctly bimodal, thus, indicating the existence of a rapid step function in axonal organelle acidification. We also show that the spatial distribution of acidified organelles along these axons is not uniform: acidified organelles are more frequent nearer the soma.

MATERIALS AND METHODS

Materials. Unless otherwise specified, all supplies were obtained from Sigma. Minimum essential medium (MEM), horse serum, Hanks' buffered saline solution (HBSS), and trypsin for astroglial cultures were obtained from GIBCO. HPTS and nigericin were obtained from Molecular Probes.

Cell Culture and Endocytic Labeling. Culture dishes for microscopy were prepared by sealing a glass coverslip over an 18-mm hole drilled in the bottom of a 60-mm plastic culture dish (17). Sympathetic neurons were obtained by dissection of ganglia from 10-day chicken embryos and cultured as described (18), except that coverslips were incubated in poly(L-lysine) at 1 mg/ml for 12–24 h and then treated for 12–24 h with laminin at 10 μg/ml. Chicken epidermal fibroblasts were

The publication costs of this article were defrayed in part by page charge payment. This article must therefore be hereby marked "*advertisement*" in accordance with 18 U.S.C. §1734 solely to indicate this fact.

Abbreviation: HPTS, 8-hydroxypyrene-1,3,6-trisulfonic acid.

prepared and grown to confluence as described (18), passaged once, and plated out at densities low enough to resolve isolated cells. Type I astroglia were obtained from dissociated embryonic day 22 or neonatal rat cerebral cortex and grown to confluence in glial maintenance medium as described by Goslin and Banker (19), passaged once, and plated at low densities on coverslips treated with poly(L-lysine) at 1 mg/ml for 1 h at 20°C. After cell attachment, medium was changed to the appropriate experimental medium: (*i*) amino acid-buffered fibroblast maintenance medium (18), (*ii*) CO_2-buffered glial maintenance medium, or (*iii*) CO_2-buffered serum-free medium containing N2 supplements (20), 1 mM sodium pyruvate, and 0.1% ovalbumin (19). For endocytic labeling, cells were incubated overnight in cell culture medium containing 2 mM HPTS and then washed thoroughly.

Generating Standard Curves for the Ratio of Fluorescence Emission Intensities at Excitation Wavelengths of 450 nm and 405 nm (F450/405) vs. pH. *In situ* standard curves were generated by ratiometric imaging of endocytically labeled cells incubated in high K^+ buffers of known pH values in the presence of the H^+/K^+ antiporter nigericin (21). For intracellular pH equilibration, 30 mM (15 mM Mes/15 mM Hepes/130 mM KCl) or 60 mM (30 mM Mes/30 mM Hepes/130 mM K^+ from KCl and KOH) pH clamp buffers were used from pH 4.5 to 8.0. Several pH points on the curve were calibrated by using a single culture dish, starting at higher pH and decreasing with successive determinations. Cells were washed twice with the appropriate pH clamp buffer and then equilibrated in buffer containing nigericin at 10 μg/ml for 20 min for the first pH point or 10 min for subsequent pH points gathered from the same dish. For each pH point on each curve, images of 10–30 labeled organelles from at least two cells were acquired for quantitative ratiometric analysis. *In vitro* standard curves were generated from fluorescence images of HPTS at 8.75 or 17.5 μM in the full range of pH clamp buffers. The microscope was focused in a plane within the solution and left in the same position, and one pair of full-field (640 × 480 pixels) images was taken for each *in vitro* data point.

Microscopy, Image Collection, Ratio Analysis, and pH Determination. Culture dishes were placed on a 37°C warmed stage of a Zeiss IM35 inverted microscope equipped with a long-working-distance condenser and a ×63 Planapochromatic objective. Visualization of all HPTS-containing organelles was achieved with 495-nm excitation/525-nm emission. A Tracor Northern Fluoroplex system (Noran Instruments, Middleton, WI) was used to provide alternating excitation at 405 nm and 450 nm for ratiometric imaging, and the emission filter was a standard fluorescein set. Images were collected via an intensified Hamamatsu charge-coupled device video camera, with the sensitivity, offset, and gain kept constant for the duration of each experiment. By using a Tracor Northern TN8500 image processing system, all images were gathered by alternate collection of 10 averaged video frames at each of the two excitation wavelengths until 50 video frames were collected and averaged for each. Background images were then digitally subtracted from the fluorescent images and labeled organelles from stored images were selected by using a binary mask. For each of the two excitation wavelengths, fluorescence intensities were measured on a numerical gray level scale of 0–255 for each pixel in an organelle image, a mean intensity for all pixels in the organelle was calculated, and these values were used to calculate a F450/405 ratio for each organelle. Organelles with saturating fluorescence intensities at either excitation wavelength were omitted from the data set. *In situ* calibration curves, generated as described above, were used to convert ratios into absolute pH values.

RESULTS

HPTS Labels Discreet Organelles and Reveals Distinct Acidic and Neutral Organelles. Cells endocytically labeled with HPTS exhibit punctate fluorescence patterns characteristic of organelle labeling when viewed by epifluorescence (Fig. 1). The absence of detectable cytoplasmic fluorescence confirms that this pyranine dye is retained in organelles, in agreement with earlier evidence of the strong retention of this pyranine dye in membrane-bound compartments (22). In addition, because the fluorescence intensity of HPTS excited at 450 nm is robust at pH 7–8 but near background at acidic pH, while the inverse is true for the fluorescence produced by 405-nm excitation, basic organelles appear bright with 450-nm excitation and dim at 405 nm, whereas acidic organelles appear bright with 405-nm and dim with 450-nm excitation, providing a qualitative indication of organelle pH (Fig. 1). In single cells exposed to HPTS for a time sufficient to label the entire endosomal–lysosomal pathway, both neutral and acidified organelles can be seen (Fig. 1 *B* and *C*).

Calibration Curves Must Be Generated *in Situ* on the Day of the Experiment for Accurate Quantitative pH Measurements of Organelles in Live Cells. To accurately quantify pH by using ratiometric imaging, the relationship between organelle pH and fluorescence ratio must be properly calibrated. We found that standard curves generated from ratiometric measurements of HPTS *in vitro* exhibited consistently higher ratios at all pH values than those generated on the same day *in situ* in endocytically labeled pH-equilibrated cells (Fig. 2), as has also been reported with the ratiometric pH probe Snarf-1 (6) and cytoplasmic HPTS (4). Thus, experimental values for organelle pH obtained with *in vitro* standard curves would be artifactually low by up to 0.5 pH unit. Calibration data gathered on different days both *in vitro* and *in situ* yielded standard curves that exhibited different ratio values in the acidic range and different slopes in the more-sensitive range between pH 6 and pH 8 (Fig. 3). In contrast, standard curves

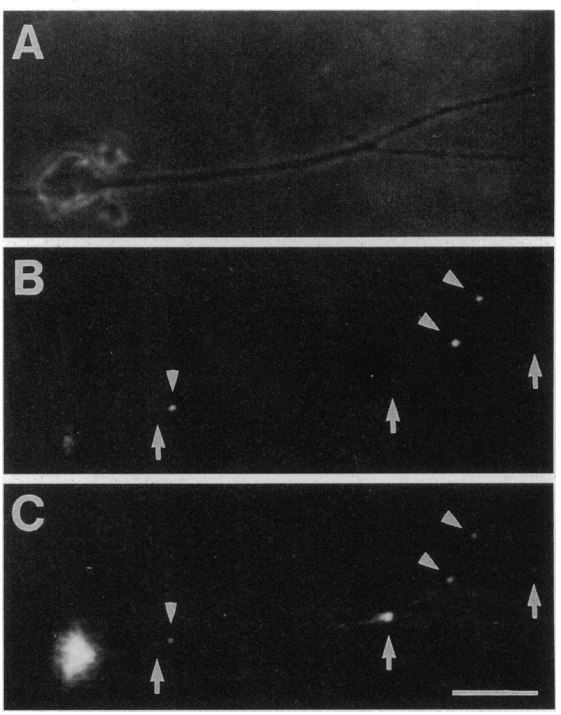

FIG. 1. Single axons contain both neutral and acidic organelles. Neuronal cultures were labeled with HPTS by endocytic uptake, and then phase contrast (*A*) and epifluorescence images obtained using 450-nm (*B*) and 405-nm (*C*) excitation light were gathered. Both acidic (arrows) and neutral (arrowheads) organelles are apparent in a single axon. (Bar = 20 μm.)

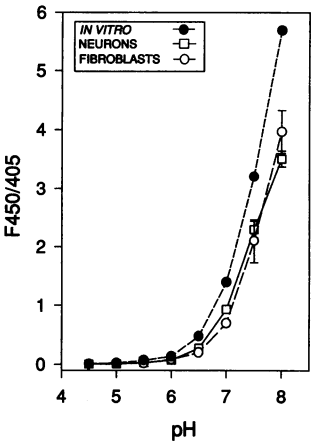

FIG. 2. Standard curves of F450/405 as a function of pH differ when determined *in vitro* vs. *in situ*. Standard curves were generated *in vitro* and *in situ* in two cell types simultaneously. F450/405 was determined for 8.75 μM HPTS in aqueous buffers of known pH (*in vitro*) or for endocytically labeled intracellular organelles that were pH clamped by incubating the cells in standard buffers containing nigericin (*in situ*). Error bars are 1 SEM.

for F450/405 vs. pH generated on the same day were essentially superimposable, except near the upper limit of HPTS sensitivity (Fig. 3). Thus, to ensure accuracy, standard curves for F450/405 vs. pH must be generated daily *in situ*, not *in vitro*.

Calibration Curves Do Not Vary with Cell Type or Medium Composition. The use of cultured neurons for *in situ* pH calibration is difficult because their processes have relatively few endocytic organelles, those in the rounded soma are difficult to resolve, and the cells wash off the coverslips easily. So, to examine the use of other cell types for calibration of neuronal experiments, standard curves using separate cultures of sympathetic neurons and epidermal fibroblasts were generated on a single day. Standard curves derived from the different cell types were virtually superimposable (Fig. 2), indicating that accessory cells can be used for experimental calibration.

Since protein and ionic environment affect the fluorescence properties of many probes (8, 16), we generated HPTS standard curves by using cultures of rat type I astrocytes grown and endocytically labeled in (*i*) amino acid-buffered L15-based medium with serum or CO_2-buffered MEM (*ii*) with or (*iii*) without serum (Fig. 4). We observed no significant difference in the curves, indicating that neither serum nor the particular type of buffering influences organelle pH measurements. Furthermore, using pH clamping buffers that differed 2-fold in their buffering capacity resulted in very similar standard curves (Fig. 4).

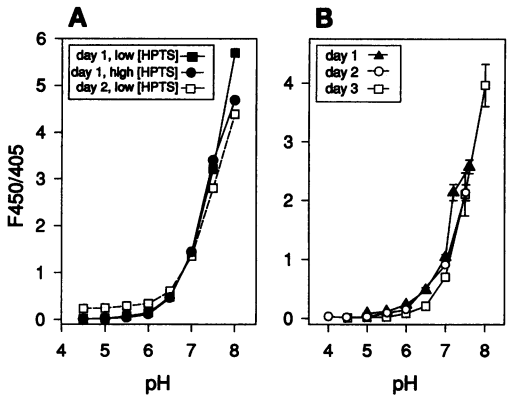

FIG. 3. Calibration curves vary from day to day. (*A*) F450/405 values were obtained *in vitro* for HPTS at concentrations of 8.75 μM and 17.5 μM in aqueous buffers of known pH on 2 days and plotted as a function of pH to generate standard curves. As seen here, these standard curves differed between days but were consistent within a single day. (*B*) *In situ* standard curves of F450/405 vs. pH generated at different times also differed. Sympathetic neurons labeled endocytically with 2 mM HPTS were pH clamped in a range of standard pH buffers. Average values of F450/405 are plotted against pH for experiments on 3 days.

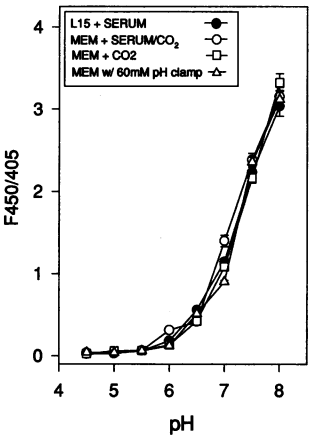

FIG. 4. Neither the composition of the labeling medium nor the strength of the pH clamping buffer significantly affects calibration. Rat type I astroglia were endocytically labeled with 2 mM HPTS overnight in medium with and without serum and with and without CO_2 buffering. For standard curve generation, images of labeled cells pH clamped in 30 mM or 60 mM buffer were collected during a single session. The mean F450/405 of organelles was plotted as a function of pH; error bars are 1 SEM.

Axons Contain Acidified Organelles in the Endocytic Pathway. Overnight steady-state labeling of the endosomal–lysosomal pathway in sympathetic cultures yielded HPTS-positive organelles throughout the axons and cell bodies. Determination of the pH of numerous individual organelles revealed that acidified organelles are found not only in the soma but also in the axon (Fig. 1). Furthermore, quantification of the relative frequency of organelle pH revealed a bimodal distribution in somatic and axonal domains (Fig. 5). Of 40 axonal organelles observed, 23 exhibited pH values of ≥6.8 and 17 exhibited pH values of ≤6.0 but not a single organelle pH fell between 6.0 and 6.8. Thus the distribution approximated two separate normal curves, which when analyzed yielded pH values of 5.42 ± 0.40 (mean ± SD) for the acidic peak and 7.38 ± 0.29 for the neutral peak. Although the bimodal distribution for somatic organelles was similar, with pH values of 5.10 ± 0.26 and 7.15 ± 0.27 (mean ± SD) for the acidic and neutral peaks, respectively, 82% of somatic organelles were

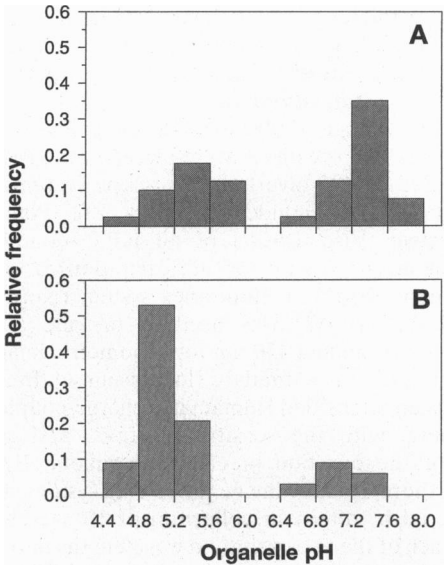

FIG. 5. Endocytically derived organelles in axons and cell bodies exhibit a bimodal frequency distribution of pH at steady state. Cultured chicken sympathetic neurons were labeled with HPTS overnight; F450/405 ratios were determined for labeled organelles and converted to pH values by comparison to an *in situ* standard curve generated at the time of the experiment in the same cell type. The histograms show the relative frequency of organelle pH for axonal (*A*) and somatic (*B*) endocytically derived organelles. (*A*) In axons, the acidic cluster of organelles exhibited a mean pH of 5.4, while the neutral cluster exhibited a mean pH of 7.4. Organelle pH values between 6.0 and 6.8 were not observed. (*B*) In neuronal cell bodies, the acidified and neutral populations exhibited mean pH values of 5.1 and 7.2, respectively. Organelle pH values between 5.6 and 6.7 were not observed.

acidic, in contrast to only 42% in axons. In addition, whereas in axons several organelles exhibited pH values between pH 5.6 and 6.0, all acidified somatic organelles exhibited pH values of <5.6.

Acidic Organelle Distribution Along Axons Is Not Uniform. To determine where in the axon endocytic organelle acidification occurs, the position of each HPTS-labeled organelle observed in axons was measured in addition to its pH. Analysis of this combined positional and pH information revealed that the distribution of the acidic organelles was not uniform (Fig. 6): the probability that an endocytic organelle was acidic correlated positively with its proximity to the soma. In the distal 100 μm of axon length, nearly all labeled organelles (86%) remained neutral, with pH > 6.8. In contrast, 44% of labeled organelles in the proximal 100 μm of axon length remained neutral and 56% were acidic, with pH < 6.0. Central regions of the axon contained intermediate proportions of acidic and neutral organelles.

DISCUSSION

Acidification is an essential element of the dynamic progression of organelle contents from predegradative endosomes and pinosomes to degradative lysosomal compartments, but its degree and course are poorly understood. In particular, the dynamics and organization of degradative processes in neuronal cells have received little experimental attention (for review, see ref. 3). In this paper, we demonstrate that acidification in the endosomal–lysosomal pathway in live neurons can be quantitatively analyzed by the proper use of a well-suited probe, HPTS. Accurate measurements require that pH calibration curves be generated *in situ*, not *in vitro*, and at the time of the experiment. This is consistent with a large body of data showing that the pH-dependent fluorescence properties of ratiometric indicators differ among soluble, intravesicular, and cytosolic states (4, 6, 8, 15, 21, 23). We also find that it is not always necessary to gather standard curve data from the experimental cell type, allowing the use of flatter more-adherent accessory cells for pH calibration in neuronal studies. By using this sensitive and accurate method, we show that axons contain acidic organelles of the endocytic pathway. Furthermore, we observe a bimodal pH distribution for endocytically labeled axonal and somatic organelles, indicating a rapid acidification step. We also demonstrate a decrease in average pH nearer the soma, suggesting a proximodistal gradient of active acidification machinery.

Although Wolfbeis *et al.* (16), in a broad study of fluorescent pH indicators, concluded that HPTS had the best spectral properties for quantitatively measuring pH in the physiologic range, and despite its use with model membrane systems, this probe has only occasionally been used for live cell studies (4, 7, 24–27). Its sulfonate and hydroxyl groups render it charged, water soluble, and highly membrane impermeant, making it impractical for studies of cytoplasmic pH but ideal for studies of the endosomal–lysosomal pathway. After entering the pathway by fluid-phase endocytosis, it remains within membrane-bounded organelles long enough to monitor protracted processes, such as the retrograde transport of axonal organelles from terminals to somata. We assert that intraorganelle pH determination using HPTS is a considerable improvement over other available methods for the study of the spatiotemporal properties of the endosomal–lysosomal pathway in live neurons and other cell types. The pH indicators that have been used for cellular studies lack the accuracy and resolution of HPTS. One commonly used class of pH indicators are the weak bases, such as acridine orange, which become protonated and accumulate in acidic organelles (28), thus offering a qualitative estimate of pH. However, treatment with an excess of non-fluorescent weak bases often fails to flush the dye out of all labeled organelles, indicating a potential lack of specificity for even relatively acidic compartments (e.g., ref. 29). Thus, it is uncertain whether fluorescent weak bases report pH or other unrelated cellular properties. Furthermore, even at subtoxic levels, these compounds can have numerous adverse effects on normal cell physiology (for reviews, see refs. 30–32).

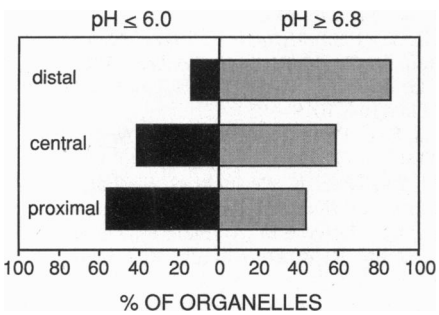

FIG. 6. Acidified endocytic organelles exhibit an uneven spatial distribution along axons. After ratiometric pH determination, the positions of 40 HPTS-labeled endocytic organelles in cultured sympathetic neuron axons were measured as a distance from either the soma or the growth cone. The fractions of acidified (pH ≤ 6.0) and neutral (pH ≥ 6.8) organelles were calculated for three regions of the axon: the distal-most 100 μm of axon, the middle portion of axon shaft >100 μm from the growth cone and the cell body, and the 100 μm of axon proximal to the soma. A greater proportion of acidified organelles was observed in more proximal regions of axons (56%) than in distal regions (14%), with an intermediate level in the middle regions (41%).

Ratiometric imaging in conjunction with *in situ* calibration can control for effects due to the intracellular environment and variable dye concentration (33). A variety of fluorescent compounds whose excitation spectra and/or fluorescence intensities change with pH have been used for such studies, but many of them, including commonly used fluorescein derivatives, are not adequate for intracellular studies (e.g., refs. 16 and 31) due to impractical spectral properties and a tendency to leak across membranes too easily for studies requiring prolonged retention of the indicator (31, 34). Although their size renders fluorescein-conjugated dextrans highly membrane impermeant and thus the best option among the fluorescein compounds for studies of the endocytic pathway (31, 34), their fluorescence properties severely limit their pH resolution and sensitivity. Because fluorescein does not have a true isosbestic point, where fluorescence is independent of pH, fluorescence intensities at the two standard excitation wavelengths of 450 nm and 490 nm vary with pH in the same direction, such that the range of fluorescence ratios obtained from the most acidic to the most basic measurable pH is small (2- to 5-fold), limiting the sensitivity and accuracy of this indicator. On the other hand, fluorescence properties are precisely what make HPTS a powerful indicator of pH in the physiologic range. HPTS has a true isosbestic point at 415 nm in the excitation spectrum, flanked by two excitation peaks whose respective emission intensities vary with pH in opposite fashion; fluorescence intensity at an excitation wavelength of 450 nm decreases with decreasing pH, but fluorescence intensity at 405 nm-excitation increases with decreasing pH. Thus, F450/405 varies >50-fold between the most acidic and the most basic pH values found in cells (31), providing at least an order of magnitude greater sensitivity to pH differences than fluorescein. This wide ratio range allows for higher resolution pH measurements and minimizes the error introduced by autofluorescence at 450-nm excitation (which can be significant with fluorescein indicators for which the ratio range is quite small) (30).

By using ratiometric imaging of cells endocytically labeled with HPTS, we observed acidified organelles within the axons of sympathetic neurons. Other studies examining endocytosis and acidification of neuronal organelles have focused predominantly on compartments involved in synaptic vesicle recycling (35, 36) or on atypical neurons such as photoreceptors, which have extremely short axon-like processes (for review, see ref.

2). Although the endosomal–lysosomal pathway in neurons has not been extensively studied, recent work localizing antigenic markers of late endosomes and lysosomes to neuronal cell bodies and proximal dendrites is consistent with the general belief that degradative activity is excluded from the axon and found only in the somatodendritic domain (37, 38), although electron microscopic evidence has suggested lysosome-like structures at nodes of Ranvier (39–41). One study of acidic compartments in neurons (38) suggested that organelles in the later stages of the endosomal–lysosomal pathway are found predominantly in the somatodendritic compartment. By combining qualitative electron microscopic methods and ratiometric imaging with fluorescein isothiocyanate-coupled inactive horseradish peroxidase, this study revealed acidic somatodendritic organelles and suggested the presence of acidic organelles in axon terminals and varicosities. However, the extremely low signal in axons, the choice of probes and their calibration in fixed cells, and compilation of calibration data from different experiments introduced important sources of error and prevented pH determination in axons.

Our data using HPTS as a ratiometric pH indicator do not contradict earlier work, but rather supplement a body of negative and largely qualitative results with positive quantitative data that change our view of the spatial organization of degradative pathways in neurons. The intense labeling by a low molecular weight free dye, the avoidance of problems associated with weak base probes, and the accurate quantification produced by calibration curves generated in live cells allowed us to determine the absolute pH of a large number of axonal organelles. These data demonstrate that while axonal organelles of the endocytic pathway remain neutral much longer than would be expected in the soma or nonneuronal cells (1), a significant fraction of them do become acidic while still within the axon. The pH of the acidified population of axonal organelles was found to average 5.4, a value considered characteristic of late endosomes (1). This indicates that at least the initial stages of acidification in the endosomal–lysosomal pathway occur within axons; it remains to be seen whether acidification is accompanied by degradative activity. Furthermore, the bimodal distribution of pH frequency suggests acidification is a rapid discreet step, such that at any time very few organelles of intermediate pH can be observed.

Along with this bimodal pH distribution, the increasing proportion of acidic organelles with increasing proximity to the soma has interesting implications for the progression of axonal organelles through the endosomal–lysosomal pathway. The uneven spatial distribution suggests an essential role for retrograde organelle transport in the acquisition of at least some lysosomal properties. We suggest two possibilities: (*i*) Golgi-derived vesicles containing the endosomal–lysosomal proton pump(s) might penetrate the axon poorly, thus making their fusion with endosomes more likely to occur in the proximal region of the axon. In this context, it is important to note the diversity of proton pumps in the cell (e.g., refs. 42 and 43). Although the proton pump associated with synaptic vesicles is present in the distal axon, it is specifically localized in a restricted region of the neuron and to a specific organelle population and is most likely targeted, transported, and regulated differently from the proton pump employed in the later stages of the endosomal–lysosomal pathway. (*ii*) Another explanation of our data is that endosomes do acquire their specific proton pumps in the distal axon but proximity to the soma increases the probability of their activation. Further study of this pathway should clarify these issues.

This paper is dedicated to the memory of Prof. Eric Holtzman. We are indebted to Dr. J. A. Swanson for helpful advice and for the use of his imaging system. This work was supported by grants from the March of Dimes Birth Defects Foundation, the National Institutes of Health, and the Harvard Mahoney Neuroscience Institute.

1. Mellman, I., Fuchs, R. & Helenius, A. (1986) *Annu. Rev. Biochem.* **55,** 663–700.
2. Holtzman, E., Augenbraun, E., St. Jules, R. & Santa-Hernandez, M. (1992) in *Endosomes and Lysosomes: A Dynamic Relationship*, eds. Storrie, B. & Murphy, R. (JAI, Greenwich, CT), pp. 225–267.
3. Parton, R. G. & Dotti, C. G. (1993) *J. Neurosci. Res.* **36,** 1–9.
4. Giuliano, K. A. & Gillies, R. J. (1987) *Anal. Biochem.* **167,** 362–371.
5. Ganz, M. B., Boyarsky, G., Sterzel, R. B. & Boron, W. F. (1989) *Nature (London)* **337,** 648–651.
6. Bassnett, S., Reinisch, L. & Beebe, D. C. (1990) *Am. J. Physiol.* **258,** C171–C178.
7. Furukawa, R., Wampler, J. E. & Fechheimer, M. (1990) *J. Cell Biol.* **110,** 1947–1954.
8. Nedergaard, M., Desai, S. & Pulsinelli, W. (1990) *Anal. Biochem.* **187,** 109–114.
9. Sasaki, S., Ishibashi, K., Nagai, T. & Marumo, F. (1992) *Biochim. Biophys. Acta* **1137,** 45–51.
10. Lee, H. C., Forte, J. G. & Epel, D. (1982) in *Intracellular pH: Its Measurement, Regulation, and Utilization in Cell Functions*, eds. Nuccitelli, R. & Deamer, D. W. (Liss, New York), pp. 135–160.
11. Swanson, J. A. (1989) *Methods Cell Biol.* **29,** 137–151.
12. Padh, H., Ha, J., Lavasa, M. & Steck, T. L. (1993) *J. Biol. Chem.* **268,** 6742–6747.
13. Sulzer, D. & Holtzman, E. (1989) *J. Neurocytol.* **18,** 529–540.
14. Kano, K. & Fendler, J. H. (1978) *Biochim. Biophys. Acta* **509,** 289–299.
15. Clement, N. R. & Gould, J. M. (1981) *Biochemistry* **20,** 1534–1538.
16. Wolfbeis, O. S., Furlinger, E., Kroneis, H. & Marsoner, H. (1983) *Fresenius Z. Anal. Chem.* **314,** 119–124.
17. Hollenbeck, P. J. & Bray, D. (1987) *J. Cell Biol.* **105,** 2827–2835.
18. Hollenbeck, P. J. (1989) *J. Cell Biol.* **108,** 2335–2342.
19. Goslin, K. & Banker, G. (1991) in *Culturing Nerve Cells*, eds. Banker, G. & Goslin, K. (MIT Press, Cambridge, MA), pp. 251–281.
20. Bottenstein, J. E. (1985) in *Cell Culture in the Neurosciences*, eds. Bottenstein, J. E. & Sato, G. H. (Plenum, New York), pp. 3–44.
21. Thomas, J. A., Buschbaum, R. N., Zimniak, A. & Racker, E. (1979) *Biochemistry* **18,** 2210–2218.
22. Straubinger, R. M., Papahadjopoulos, D. & Hong, K. (1990) *Biochemistry* **29,** 4929–4939.
23. Owen, C. S. (1992) *Anal. Biochem.* **204,** 65–71.
24. Furukawa, R., Wampler, J. E. & Fechheimer, M. (1988) *J. Cell Biol.* **107,** 2541–2549.
25. Martinez, R., Gillies, R. J. & Giuliano, K. A. (1988) *J. Cell. Physiol.* **136,** 154–160.
26. Daleke, D. L., Hong, K. & Papahadjopoulos, D. (1990) *Biochim. Biophys. Acta* **1024,** 352–366.
27. Lee, K.-D., Nir, S. & Papahadjopoulos, D. (1993) *Biochemistry* **32,** 889–899.
28. Schuldiner, S., Rottenberg, H. & Avron, M. (1972) *Eur. J. Biochem.* **25,** 64–70.
29. Hollenbeck, P. J. (1993) *J. Cell Biol.* **121,** 305–315.
30. Holtzman, E. (1989) in *Lysosomes*, eds. Anonymous (Plenum, New York), pp. 243–317.
31. Tsien, R. Y. (1989) *Methods Cell Biol.* **30,** 127–156.
32. Palmgren, M. G. (1991) *Anal. Biochem.* **192,** 316–321.
33. Bright, G. R., Fisher, G. W., Rogowska, J. & Taylor, D. L. (1987) *J. Cell Biol.* **104,** 1019–1033.
34. Ohkuma, S. & Poole, B. (1978) *Proc. Natl. Acad. Sci. USA* **75,** 3327–3331.
35. Matteoli, M., Takei, K., Perin, M. S., Südhof, T. C. & De Camilli, P. (1992) *J. Cell Biol.* **117,** 849–861.
36. Mundigl, O., Matteoli, M., Daniell, L., Thomas-Reetz, A., Metcalf, A., Jahn, R. & De Camilli, P. (1993) *J. Cell Biol.* **122,** 1207–1221.
37. Parton, R. G., Simons, K. & Dotti, C. G. (1992) *J. Cell Biol.* **119,** 123–137.
38. Augenbraun, E., Maxfield, F. R., St. Jules, R., Setlik, W. & Holtzman, E. (1993) *Eur. J. Cell Biol.* **61,** 34–43.
39. Berthold, C.-H. & Mellström, A. (1986) *Neuroscience* **19,** 1349–1362.
40. Gatzinsky, K. P., Berthold, C.-H. & Corneliuson, O. (1988) *J. Neurocytol.* **17,** 531–544.
41. Gatzinsky, K. P. & Berthold, C.-H. (1990) *J. Neurocytol.* **19,** 989–1002.
42. Nelson, N. (1992) *J. Exp. Biol.* **172,** 19–27.
43. Forgac, M. (1992) *J. Bioenerg. Biomembr.* **24,** 341–350.